PHYSICAL REVIEW C

NUCLEAR PHYSICS

THIRD SERIES, VOLUME 30, NUMBER 3 SEPTEMBER 1984

Proton resonances in ^{28}Si from $E_x = 13.4$ to 14.5 MeV

R. O. Nelson, E. G. Bilpuch, and C. R. Westerfeldt
Duke University, Durham, North Carolina 27706
and Triangle Universities Nuclear Laboratory, Duke Station, Durham, North Carolina 27706

G. E. Mitchell
North Carolina State University, Raleigh, North Carolina 27695
and Triangle Universities Nuclear Laboratory, Duke Station, Durham, North Carolina 27706

(Received 11 April 1984)

The ^{27}Al(p,p$_0$), (p,p$_1$), (p,p$_2$), (p,α_0), and (p,α_1) excitation functions were measured at 90°, 105°, 135°, and 160° in the range $E_p = 1.85$–3.05 MeV with an overall resolution of 350–400 eV full width at half maximum. Resonance parameters were extracted for 73 resonances with a multilevel, multichannel R-matrix analysis code; these parameters include resonance energy, total angular momentum, partial widths, and channel spin and orbital angular momentum mixing ratios. Eight analog states were identified, and the Coulomb displacement energies and spectroscopic factors were calculated. The values of the s-wave strength functions for $J=2$ and 3 are $S_{J=2}=0.042$ and $S_{J=3}=0.012$. The spectroscopic strengths of the $J^\pi = 4^-$, 5^-, and 6^- particle-hole states are presented and compared with other results.

I. INTRODUCTION

This paper presents results from an extensive study of proton resonances in ^{28}Si. A recent paper[1] described the results in the range $E_p = 0.92$–1.85 MeV, while a preliminary value for the width of the 6^-, $T=1$ state in ^{28}Si was reported earlier.[2] Here the measurement and analysis of the ^{27}Al(p,p$_0$), (p,p$_1$), (p,p$_2$), (p,α_0), and (p,α_1) resonance reactions are described for the range $E_p = 1.85$ –3.05 MeV. Seventy-three resonances were observed and analyzed in this energy range with an overall resolution of 350 to 400 eV (FWHM). Although the analysis of these data involves numerous possible mixings and up to seven resonance angular momenta, most of the resonances were successfully analyzed with little remaining ambiguity.

Only two previous elastic scattering studies have been performed in the range $E_p = 1.85$–3.05 MeV. An early experiment with good energy resolution but with no analysis was performed by Shoemaker *et al.*,[3] while in a more recent poor resolution experiment a few resonances in this range were analyzed by Rahman *et al.*[4] The (p,α) reaction has been studied with poor resolution by Abuzeid *et al.*,[5] Zolnai *et al.*,[6] and Hsu *et al.*[7] Resonance angular momenta and parities were determined for some of the resonances observed in the (p,α) reactions. Studies of the (p,γ) reaction by Meyer *et al.*[8] and of the (p,γ), (p,p'γ), and (p,$\alpha\gamma$) reactions by Dalmas[9,10] provided information on the energies, total widths, decay strengths, and some of the resonance angular momenta in this energy range. The data as of 1978 were summarized by Endt and Van der Leun.[11] The present results provide the partial widths, total widths, mixing ratios, orbital angular momenta, and many of the resonance spins. The equipment and procedures are described in Sec. II and the analysis and spectroscopic results are presented in Secs. III and IV. A discussion of analog states is given in Sec. V.

The spin dependence of s-wave neutron (or proton) strength functions may be used to infer an optical model spin-spin potential energy term.[12] The 25 nonanalog, s-wave resonances in ^{28}Si for which spins were uniquely determined form the largest such data set for proton scattering. The s-wave strength functions are presented in Sec. VI.

Several papers providing information on the 6^-, $T=1$ state in ^{28}Si have been published since our preliminary report of the proton width. Our value for Γ_p is in good agreement with the value obtained by Snover *et al.*[13] from a study of the (p,γ) reaction. In Sec. VII we discuss the implications of our data for some of the current theories on the quenching of the single particle strength of the 6^- state. Comparisons are also made with the strength observed in other reactions.

II. EXPERIMENT

The experiment was performed with the upgraded model KN Van de Graaff accelerator and the associated

high resolution system at Triangle Universities Nuclear Laboratory (TUNL). This system has been described elsewhere.[14,15] Targets consisted of 0.6 to 1.4 $\mu g/cm^2$ Al evaporated onto 5 $\mu g/cm^2$ C foils. Data were taken in steps of 100 to 600 eV. The experimental procedures are described in Ref. 1.

The scattered protons and alpha particles were detected by Si surface barrier detectors at laboratory angles of 90°, 105°, 135°, and 160°. The alpha particles which decay to the first excited state of ^{24}Mg have almost the same energy as the protons elastically scattered from ^{16}O. In order to observe the α_1 decay, three 40 μm thick transmission surface barrier detectors were placed opposite the proton detectors at laboratory angles of 120°, 135°, and 150°. Protons with energies greater than 2.4 MeV are not completely stopped in these thin detectors, thus permitting separation of the p_0 and α_1 peaks at bombarding energies above 2.4 MeV. At lower energies the very small penetrabilities inhibit α_1 decay. The α_0 decay was monitored in the transmission detectors to provide normalization of the yields of the two sets of detectors.

III. ANALYSIS

For proton scattering from ^{27}Al at energies below 3.05 MeV there are ten open particle channels: elastic scattering, inelastic scattering to the first five excited states of

TABLE I. Allowed channels for proton resonances in ^{28}Si. * indicates decay is kinematically inhibited. ** indicates decay is forbidden by conservation of parity.

	p_0		p_1		p_2		α_0		α_1	
J^π	l	s	l	s	l	s	l	s	l	s
0^+	2	2	0	0	2	2	0	0	2	2
0^-	3	3	1	1	1	1	**		**	
1^+	2	2	0	1	0	1	**		2	2
	2	3	2	1	2	1				
					2	2				
1^-	1	2	1	0	1	1	1	0	1	2
	3	2	1	1	1	2			3	2
	3	3			3	2				
2^+	0	2	2	0	0	2	2	0	0	2
	2	2	2	1	2	1			2	2
	2	3			2	2				
2^-	1	2	1	1	1	1	**		1	2
	1	3	3	1	1	2			3	2
	3	2			3	1				
	3	3			3	2				
3^+	0	3	2	1	2	1	**		2	2
	2	2			2	2				
	2	3								
3^-	1	2	3	0	1	2	3	0	1	2
	1	3	3	1	3	1			3	2
	3	2			3	2				
	3	3								
4^+	2	2	*		2	2	4	0	2	2
	2	3								
4^-	1	3	3	1	3	1	**		3	2
	3	2			3	2				
5^+	2	3	*		*		**		*	
5^-	3	2	*		3	2	5	0	3	2
	3	3								
6^-	3	3	*		*		**		*	

^{27}Al, and alpha decay to the ground state and first three excited states of ^{24}Mg. Only the p_0, p_1, p_2, α_0, and α_1 channels have strong decay for $E_p < 3$ MeV. The other particle channels and the capture channels were neglected in the analysis.

Resonance spin angular momenta up to 7 and l values up to 4 were considered in the elastic scattering analysis. Since no $l=4$ strength was observed, we neglect $l=4$ elastic scattering in our discussion. The combinations of channel spins and l values considered for the observed channels are listed in Table I for each J^π. For example, a $J^\pi = 1^+$ resonance has two elastic scattering channels, $l=2$ ($l=4$ is neglected) with $s=2$ or 3, and thus channel spin mixing can occur. For a $J^\pi = 2^-$ resonance there are four possible elastic channels, $l=1$ or 3 with $s=2$ or 3, allowing both channel spin mixing and l mixing. The four possible partial widths for elastic or inelastic proton scattering may be expressed in terms of the total elastic or inelastic proton width, a channel spin mixing ratio, and two l-mixing ratios. Channel spin mixing and l mixing can occur for proton channels, while only l mixing can occur for α_1 decay. No mixing is possible for α_0 decay. In addition, α_0 decay occurs only for natural parity states.

The channel spin mixing ratios are defined for the nth proton decay channel as

$$\xi_n = \sum_l \Gamma_{p_n,s_>,l}/\Gamma_{p_n} , \tag{1}$$

where $s_>$ is the higher channel spin and Γ_{p_n} is the total width in the nth decay channel. The l-mixing ratios are defined as

$$\epsilon_{ns} = \pm(\Gamma_{p_n,s,l+2}/\Gamma_{p_n,s,l})^{1/2} . \tag{2}$$

For convenience we define the corresponding mixing angles ψ_{ns} as

$$\tan(\psi_{ns}) = \epsilon_{ns} . \tag{3}$$

The subscript n is omitted for the elastic scattering mixing ratios. A similar l-mixing ratio can be defined for the α_1 channel, but no l mixing was observed in the α_1 decay. In all cases the range of ξ is from 0 to 1, and the range of ψ is from $-90°$ to $+90°$.

Due to very small penetrabilities, the observation of decay with higher l values and therefore of strong l mixing is extremely reduced at the lower energies. At higher energies larger l-mixing ratios are possible, but on the average the lower l values should dominate by the ratio of the l and $l+2$ penetrabilities. In practice, determination of l mixing was difficult because the l-mixing ratios were extremely small at low energies, and at higher energies interference between resonances made determination of mixing much more difficult. For nonelastic decay the amount of l mixing could not be determined from the present measurements; the lowest possible l values were used in fitting the data.

In contrast, channel spin mixing is not dominated by such kinematic effects. Correspondingly, a wide variety of channel spin mixing ratios is observed over the entire energy range. When the entrance mixing was determined from the elastic scattering data, the inelastic channel spin mixing ratio could often be determined from the inelastic angular distribution.

The data were fit with an R-matrix[16] based computer program.[15] The fitting procedure has been described previously, and examples of the determination of resonance angular momenta and mixing ratios have been given.[1,17] All decay channels were fit simultaneously. Parameters for all resonances were included in the final fit, including the parameters in the lower energy region (0.92—1.85 MeV) and a qualitative fit to several large resonances above 3.05 MeV. Although data were measured up to 3.4 MeV, the large number of overlapping levels at higher energies made the fitting procedure extremely difficult. In addition, as one approaches the top of the Coulomb barrier the approximation of the background as Rutherford plus hard sphere scattering is no longer valid. This is apparent in the poorer fits obtained at the higher energies.

Our multilevel, multichannel, R-matrix analysis program was expanded to allow simultaneous fitting of five particle groups with numerous possible combinations of angular momenta. This analysis was made feasible by the new VAX 11/780 computing facilities at TUNL including the associated graphics terminals and software.[18]

IV. DATA

The 160° data and fit are presented in Figs. 1 and 2, where the solid line is the R-matrix fit to the data. The extracted resonance parameters are listed in Tables II—IV. Total reduced widths γ_p^2 are defined as

$$\gamma_p^2 = \sum_{s,l} \Gamma_{p,s,l}/2P_l , \tag{4}$$

where the Coulomb penetrability, P_l, is calculated from the Coulomb wave functions evaluated at a channel radius $R_c = 1.25(1+A^{1/3})$ fm.

The fits in the energy range from 1.85 to 2.4 MeV are very good. The data were normalized to the fit in this region. Above 2.4 MeV the number of overlapping levels,

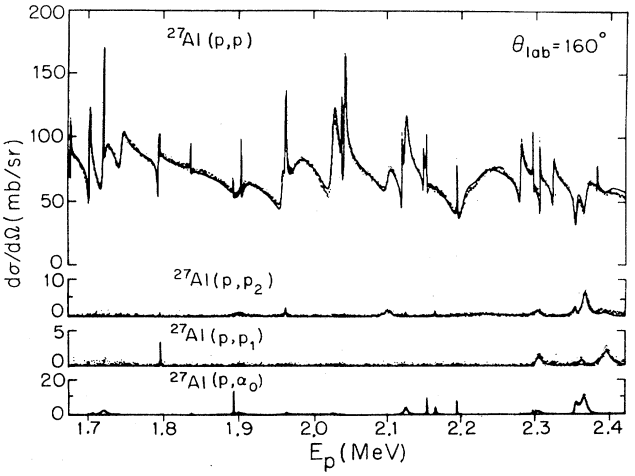

FIG. 1. The 160° data and fit in the range $E_p = 1.67$—2.42 MeV. The solid line is the R-matrix fit to the data. Uncorrected laboratory energies are plotted.

TABLE II. Resonance parameters for ^{27}Al(p,p) and ^{27}Al(p,α_0).

E_p[a] (MeV)	J^{π}[b]	l[c]	ξ	ψ_2[d] (deg)	ψ_3[d] (deg)	Γ_p[e] (keV)	γ_p^2[f] (keV)	l_{α_0}	Γ_{α_0}[e] (keV)	$\gamma_{\alpha_0}^2$[f] (keV)
1.8981	4^+	2	0.15			0.060	2.5	4	0.080	21.
1.9060	1^-	1	0.0	0		19.	124.	1	0.80	6.2
1.9090	5^+	2				0.080	3.3			
1.9637	2^-	1	0.0	0		4.0	23.			
1.9680	2^+	0	0.15	0		1.4	9.9	2	0.040	0.58
1.9774	3^-	1	0.90	0	0	31.	173.	3	1.0	45.
2.0329	2^+	0	0.05	0		8.5	32.	2	0.15	1.8
2.0450	$5(4)^+$	2				0.15	4.4			
2.0485	3^+	0	0.95[h]		0	1.8	7.0			
2.1069	2^-	1	0.05	0	0	11.	49.			
2.1262	3^+	0	0.80[h]		0	0.57	3.8			
2.1308	2^+	0	0.0	15		5.0	16.	2	0.65	6.3
2.1313	$(1^-,2^+)$	0	0.0	0		0.12	0.21			
2.1549	$(3,4)^-$	1	1.0[h]		+30	0.45	35.			
2.1595	4^+	2	0.50			0.17	3.9	4	0.08	9.7
2.1711	2^+	0	0.30	10		0.43	3.4	2	0.90	8.0
2.2002	$2(3)^+$	2	g	90		0.50	10.4			
2.2003	4^+	2	0.25			0.04	0.83	4	0.15	16.
2.2056	3^-	1	0.6	0	0	20.	75.			
2.2293	1^-	1	0.0	0		35.	126.			
2.2860	3^-	1	0.10[i]	0	90	2.7	54.			
2.3032	4^+	2	0.0			0.15	2.5	4	0.007	0.58
2.3105	1^-	1	0.0	0		2.0	6.3	1	1.7	5.5
2.3120	3^+	0	1.0		0	0.32	0.46			
2.3300	$(3,4)^-$	1	0.95[i]		0	2.2	34.			
2.3607	3^-	1	0.65	0	0	2.5	7.4	3	1.4	2.4
2.3731	3^-	1	0.05	0	0	4.7	14.	3	2.4	40.
2.3902	$(3-6)^-$	3	g			0.035	5.2			
2.4030	1^-	1	0.0	0		2.5	6.9	1	0.20	0.55
2.4418	2^+	0	0.0	−20		2.2	5.1	2	3.0	15.
2.4716	4^+	2	0.40			0.050	0.60	4	0.20	11.
2.4751	2^+	0	0.25	0		1.5	6.2	2	1.0	4.7
2.4827	$4(5)^+$	2	0.15			2.6	31.			
2.4872	5^-	3	0.75			0.30	38.			
2.4883	2^+	2	0.0	90		0.30	3.6	2	0.080	0.37
2.5172	4^+	2	1.0			0.080	0.91	4	0.005	0.24
2.5304	1^-	1	0.0	0		3.0	7.0			
2.5436	$3(2)^-$	1	1.0		0	45.	105.			
2.5553	$5(4)^+$	2				1.2	13.			
2.5560	2^+	0	0.20[h,i]			2.4	6.5			
2.5728	2^+	0	0.50	0		4.0	23.	2	1.8	7.0
2.5829	(2^-)[j]	1	0.40	0	0	36.	79.			
2.5975	3^-	1	0.50	0	0	1.2	2.6	3	3.0	31.
2.6030	1^+	2	1.0			1.0	9.8			
2.6044	4^+	2	0.0			0.15	1.5	4	0.60	24.
2.6138	5^-	3	1.0			0.20	19.	5	0.040	8.4
2.6703	$4(3)^-$	1	1.0		+15	13.	110.			
2.7132	3^+	0	1.0		0	0.80	0.78			
2.7216	4^+	2	0.0			1.0	8.2			
2.7234	(2^-)[j]	1	1.0		0	3.0	5.6			
2.7263	5^+	2				0.60	4.9			
2.7410	3^+	0	0.60[i]		50	1.4	8.6			
2.7592	$(3)^-$[j]	1	1.0		0	35.	63.			
2.7620	2^+	0	0.0	0		25.	23.	2	0.90	2.5
2.8099	2^+	0	0.0	0		0.60	0.54	2	0.20	0.52
2.8148	4^+	2	0.0			0.20	1.4	4	1.2	30.
2.8226	(1^-)[j]	1	0.0	0		40.	68.			
2.8458	4^+	2	0.70			0.17	1.2	4	0.38	8.9
2.8505	$(4,5)^+$	2	g			0.070	0.47			

TABLE II. (*Continued*).

E_p[a] (MeV)	J^{π}[b]	l[c]	ξ	ψ_2[d] (deg)	ψ_3[d] (deg)	Γ_p[e] (keV)	γ_p^{2}[f] (keV)	l_{α_0}	Γ_{α_0}[e] (keV)	$\gamma_{\alpha_0}^{2}$[f] (keV)
2.8676	4^-	1	1.0		+ 10	2.3	9.4			
2.8750	6^-	3				3.7	209.			
2.8765	4^+	2	0.50			0.85	5.5	4	2.1	46.
2.8770	(2^-)[j]	1	0.40	0	0	17.	27.			
2.8942	2^+	0	0.0[i]	0		16.	14.	2	0.60	1.4
2.9110	3^+	0	0.85		0	0.36	0.62			
2.9113	(0^+)[j]	2				1.0	6.2			
2.9207	$(3-5)^-$	3	0.50			0.11	6.0			
2.9556	3^+	0	1.0		25	19.	31.			
2.9968	$(5,6)^-$	3				0.18	8.5			
3.0171	2^+	0	0.0[i]	0		6.0	4.7	2	15.	29.
3.0171	3^+	0	0.85		0	5.6	7.1			
3.0397	3^-	3	0.10	90	90	0.30	13.	3	0.10	0.45
3.0483	3^-	1	0.0	0		0.80	1.1	3	10.	45.

[a]Laboratory energies are listed. Except for very large resonances, absolute energies should be accurate within 3 keV.
[b]Spin assignments have been listed according to the following convention: 2^+, definite spin and parity; $2(3)^+$, definite l value, preferred spin outside of parentheses; $(2,3)^+$, definite l value, spin not completely determined; (2^+) possible l value and J^{π}. Resonance parameters correspond to the preferred spin or the highest spin listed. A complete list of parameters is available upon request.
[c]For ψ_2=90° with ξ=0.0, or ψ_3=90° with ξ=1.0, or ψ_2=ψ_3=90°, the higher l value is listed.
[d]When determined, the relative phase is indicated by + or −.
[e]See text for errors in widths.
[f]Total reduced widths are calculated according to Eq. (4).
[g]Parameter is undetermined for this resonance.
[h]Two or more sets of mixing ratios and widths gave acceptable fits.
[i]Assignments for ξ, ψ_2, and ψ_3 are uncertain due to strong interference effects. Other solutions may be possible.
[j]Probable l value and possible J^{π} to fit strong inelastic decay.

interference, and errors in the background determination made fitting much more difficult. The data normalizations for the higher energy region were assumed the same as those in the lower energy region, except for changes due to differing target thicknesses. A satisfactory fit to the p_2 excitation curve near 2.8 MeV was not obtained due to the difficulty in determining the number of levels which contribute to the anomaly, and in obtaining the l values, spins, and relative phases of some of the levels. A minimum of 11 levels with p_2 decay were identified in the region from 2.7 to 2.9 MeV. Although more decay channels and resonances were included in the final fit, our preliminary value of Γ_p=3.7 keV for the 6^-, T=1 resonance at E_p=2.875 MeV remains unchanged. The problem in fitting the elastic scattering background at higher energies is apparent in Fig. 2.

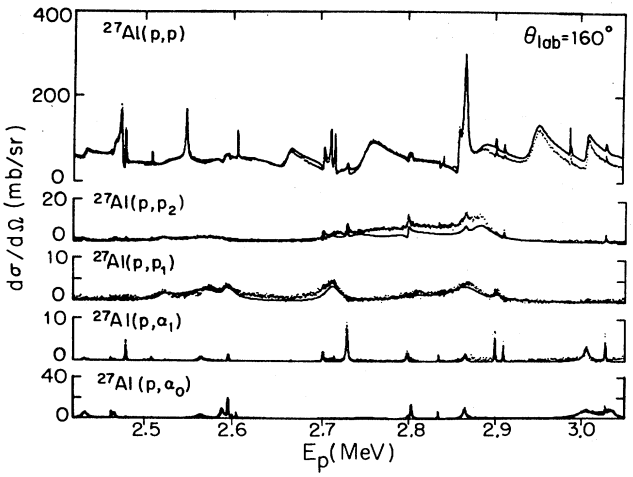

FIG. 2. The 160° data and fit in the range E_p=2.42–3.05 MeV. The solid line is the R-matrix fit to the data. The (p,α_1) data were taken at 150°. Uncorrected laboratory energies are plotted.

The resonance energies should be accurate within 3 keV. Errors in the widths are typically 10% for widths larger than 300 eV and 20% for widths less than 300 eV. The errors in ξ and ψ depend on the width, l value, and total angular momentum of a resonance. Typical errors in ξ are ±0.15, while typical errors in ψ are ±15°. Individual errors may vary considerably from these values, especially in regions with many overlapping resonances.

Meyer *et al.*[8] observed 27 resonances in the ^{27}Al(p,γ) reaction between 1.85 and 2.5 MeV. Four of these resonances were not observed in the present experiment, although 11 additional levels were found. Four of these additional levels are members of previously unresolved doublets. Our spin assignments agree with the possible values listed by Meyer *et al.* with the exception of four states. The 2.303 MeV level was assigned $J^{\pi}=2^+$ by Meyer while we find $J^{\pi}=4^+$ from the elastic scattering data and the α_0 angular distribution. The resonances at E_p=2.312 and 2.483 MeV were both assigned $J^{\pi}=(2^+,3^-)$ by

TABLE III. Resonance parameters for ^{27}Al(p,p_1) and ^{27}Al(p,p_2).

E_p[a] (MeV)	J^π	l_{p_1}	ξ_{p_1}	Γ_{p_1} (keV)	$\gamma_{p_1}^2$ (keV)	l_{p_2}	ξ_{p_2}	Γ_{p_2} (keV)	$\gamma_{p_2}^2$ (keV)
1.9060	1^-					1	b	0.60	308.
1.9680	2^+					0	1.0	0.080	6.7
2.1069	2^-					1	0.70	0.35	46.
2.1313	$(1,2^-)$					0	1.0	0.40	11.
2.1711	2^+					0	1.0	0.27	7.1
2.2293	1^-					1	b	1.4	97.
2.3105	1^-	1	b	2.0	48.	1	b	2.0	95.
2.3607	3^-					1	1.0	0.30	12.
2.3731	3^-					1	1.0	1.1	40.
2.4030	1^-	1	b	8.0	140.	1	b	3.0	98.
2.4418	2^+					0	1.0	0.60	5.4
2.4751	2^+					0	1.0	0.15	1.2
2.4883	2^+					0	1.0	0.15	1.2
2.5172	4^+					2	1.0	0.010	1.8
2.5304	1^-	1	b	6.5	79.	1	b	6.5	135.
2.5829	$(2)^-$	1	1.0	7.0	74.	1	0.50	4.0	70.
2.5975	3^-					1	1.0	0.10	1.7
2.6030	1^+	0	1.0	11.	41.				
2.7132	3^+					2	1.0	0.20	18.
2.7234	$(2)^-$	1	1.0	12.	90.	1	0.90	5.0	58.
2.7410	3^+					2	b	0.10	8.0
2.7592	$(3)^-$					1	1.0	6.0	63.
2.8099	2^+					0	1.0	0.80	2.8
2.8226	$(1)^-$	1	b	9.0	55.	1	1.0	25.	226.
2.8765	4^+					2	1.0	0.40	21.
2.8770	$(2)^-$	1	1.0	16.	87.	1	1.0	10.	79.
2.8942	2^+					0	1.0	10.	29.
2.9113	(0^+)	0	0.0	8.0	17.				
2.9207	$(3-5)^-$					3	1.0	0.19	128.
3.0397	3^-					1	1.0	0.20	1.1

[a]Conventions are the same as in Table II. The l-mixing angles for inelastic decay are undetermined. $\psi=0$ is assumed.
[b]Parameter is undetermined for this resonance.

TABLE IV. Resonance parameters for ^{27}Al(p,α_1).

E_p[a] (MeV)	J^π	l_{α_1}	Γ_{α_1} (keV)	$\gamma_{\alpha_1}^2$ (keV)
2.4418	2^+	0	0.20	18.
2.4716	4^+	2	0.020	6.6
2.4883	2^+	0	0.40	30.
2.5172	4^+	2	0.005	1.4
2.5728	2^+	0	0.30	16.
2.6044	4^+	2	0.08	15.
2.7132	3^+	2	0.10	12.
2.7410	3^+	2	0.60	67.
2.8099	2^+	0	0.40	9.2
2.8226	$(1)^-$	1	0.10	3.4
2.8458	4^+	2	0.070	5.3
2.8765	4^+	2	0.10	6.8
2.9110	3^+	2	0.20	12.
2.9207	$(3-5)^-$	3	0.13	27.
3.0171	2^+	0	2.0	8.4
3.0171	3^+	2	0.30	12.
3.0397	3^-	1	0.35	6.0

[a]Conventions are the same as in Table II. The l mixing angle ψ is undetermined for the (p,α_1) reaction. $\psi=0$ is assumed.

Meyer. The former was determined to have $J^\pi=3^+$ from the elastic scattering data, and the latter has $J^\pi=4,(5)^+$. For the 2.403 MeV resonance we assign $J^\pi=1^-$ on the basis of the elastic scattering and the (p,α_0) data. This assignment is in disagreement with the $J^\pi=(2,3^-)$ assignment of Meyer *et al.* Most of these discrepancies are for states with weak gamma decay where other levels may overlap. All of our energies agree within 3 keV with those of Meyer *et al.*

Dalmas[9,10] has obtained resonance energies, total widths, and decay strengths for 83 resonances in the range $E_p=1.95-3.05$ MeV. Correspondence was established for about 80% of our resonances. Most of our energies agree with those of Dalmas within 3 keV, except for some very broad resonances for which a precise energy determination is difficult. A few of the broad resonances which were analyzed in the present study as single resonances with both p_1 and p_2 decay are attributed to two separate levels by Dalmas. Most of the total widths and decay strengths measured in the two experiments are in good agreement, although many of the p_1, p_2, and α_1 decays listed by Dalmas are too weak to be observed in the present experiment.

The gamma decay of the 6^-, $T=1$ state has been studied through the (p,γ) reaction by Neal and Lam,[19] Miehe *et al.*,[20] Neal and Chagnon,[21] and Snover *et al.*[13] Upper limits on the nonelastic decay of the 6^- state are reported by Snover *et al.*

V. ANALOG STATES

The identification of analog states for odd-mass targets in our mass range has been discussed previously.[17] Eleven analog states were identified in the range E_p=0.92–1.85 MeV.[1] In the range of energies covered here 12 states are known in ^{28}Al from (d,p) studies.[11] For the states in ^{28}Al at E_x=4.77, 4.93, 5.00, and 5.14 MeV no analog states could be identified. The only resonance previously identified as an analog state in our energy range is the E_p=2.876 MeV (E_x=14.36 MeV) $J^\pi=6^-$ resonance which is the analog of the E_x=5.17 MeV level in ^{28}Al.

Table V lists the Coulomb energies, (d,p) and proton spectroscopic factors, and energies of the parent and analog states. We define the proton spectroscopic factor $C^2S_p=\Gamma_p/\Gamma_{sp}$, where C^2 is the usual isospin Clebsch-Gordan coefficient. For ^{27}Al(p,p), $C^2=\frac{1}{2}$. The proton single particle widths Γ_{sp} were calculated by the method of Harney and Weidenmüller.[22] The diffuseness and radius parameters of the potential well were the same as those used in the (d,p) analyses.[23–25] The proton single particle widths are averages of the values calculated for the two possible particle angular momenta. The individual single particle widths varied less than 12% from their average value. Due to penetrability effects, determination of the spectroscopic factor for l-mixed resonances is less certain for higher l values than for lower l values.

For the E_x=4.69 MeV state in ^{28}Al and its analog, the dominant l value is not the same in the (d,p) and resonance analyses, but similar discrepancies have been noted for the lower energy analog states.[1] The analog strength of the E_x=4.74 MeV state may be split between the two resonances at E_p=2.483 and 2.517 MeV. The 2.517 MeV resonance was previously identified as the analog on the basis of (p,γ) measurements by Rahman *et al.*,[26] while we assign the 2.483 MeV level as the analog state based on the better agreement of the (d,p) and proton spectroscopic factors and the α_0 decay of the 2.517 MeV resonance. In some cases, such as the state at E_x=4.69 MeV, only the l values, spins, and Coulomb energies were used in the identification process due to the poor mutual agreement of the two (d,p) spectroscopic factors.

VI. s-WAVE STRENGTH FUNCTIONS

A difference in s-wave strength functions for states of different angular momenta may indicate the existence of spin-exchange forces in the nucleon-nucleon interaction.[12] To search for spin-spin effects, neutron or proton scattering from odd-odd or odd-mass targets must be studied because only one J value is allowed in s-wave scattering from even-even targets.

Neutron s-wave strength functions have been extracted from measurements[12] of isolated resonances and more recently from spin-spin cross sections in a region of overlapping resonances.[27] Poor statistics and possible intermediate structure effects complicate the interpretation of these results.

The present data allow the extraction of the proton s-wave strength functions for resonances with $J=2$ and 3 in ^{28}Si. A total of 33 s-wave resonances were observed in the energy range E_p=0.92–3.05 MeV. Definite spin assignments could not be made for two of these resonances. In addition, there are six analog states identified in this region. Omission of these eight states leaves 25 nonanalog states with definite spin assignments.

The reduced widths and their sums are plotted in Fig. 3. No anomalous effects are evident in the plots. The strength function is $S=\langle\gamma^2\rangle/D$, where $\langle\gamma^2\rangle$ is the average reduced width and D is the average level spacing. An

TABLE V. Analog state parameters in ^{28}Si.

J^π	E_x[a] (MeV)	l	E_p^{lab} (MeV)	E_C (MeV)	Γ_{sp}[b] (keV)	Γ_p[c] (keV)	S_p	S_{dp}[d]	S_{dp}[e]
5^+	4.31	2	1.909	5.257	16.8	0.080	0.010	0.056	0.065
$5,(4)^+$	4.46	2	2.045	5.237	24.	0.15	0.013	0.033	0.038
3^-	4.69	1	2.286	5.240	218.	2.7	0.025	0.31	0.17
		3			3.4	0.23	0.14	0.079	0.30
4^+	4.74	2	2.483	5.379	54.	2.6	0.096	0.062	0.080
1^+	4.85	2	2.603	5.385	66.	1.0	0.030	0.10	
2^-	4.91	1	2.583	5.306	306.	36.	0.24	0.24	0.14
		3			6.4	<2.0	<0.63	0.060	0.32
3^+	5.02	0	2.713	5.321	608.	0.80	0.003	0.006	0.003
		2			82.	<0.060	<0.002	0.009	0.017
6^-	5.17	3	2.875	5.327	11.9	3.7	0.62	0.65[f]	

[a]Excitation energies of the parent states in ^{28}Al from Ref. 11.
[b]Values of Γ_{sp} are averaged over the possible particle angular momenta.
[c]Upper limits for widths are determined from the fitting procedure.
[d]Reference 23.
[e]Reference 24.
[f]Reference 25.

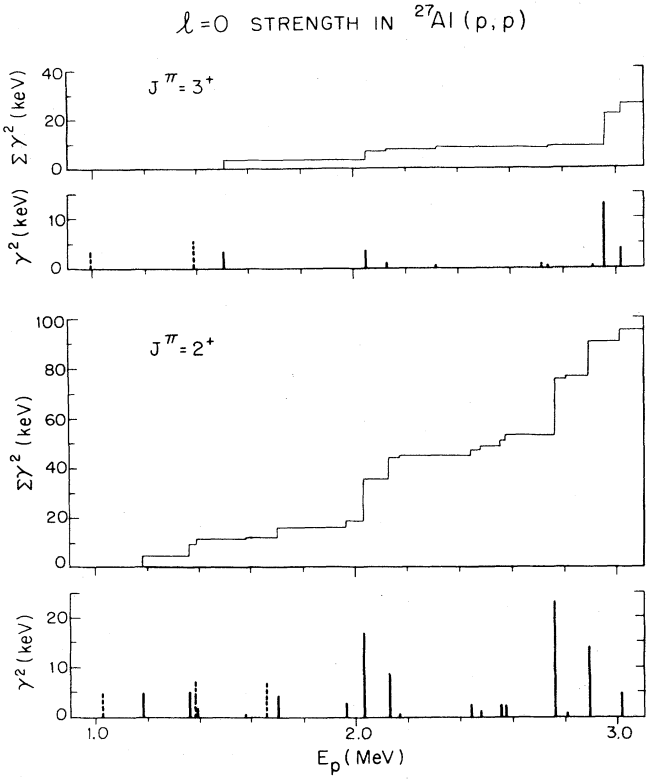

FIG. 3. The s-wave reduced widths and their sums versus energy. Analog states (dashed lines) are omitted from the sums. No anomalous effects are evident.

equivalent definition is

$$S=(N-1)\sum_i \gamma_i^2/N\Delta E\ ,$$

where N is the sample size and ΔE is the energy range of the sample. The strength function calculated from 17 $J=2$, $l=0$ resonances in ^{28}Si is $S_{J=2}=0.042\pm0.014$, while the strength function for the eight $J=3$ resonances is $S_{J=3}=0.012\pm0.006$. The fractional statistical error for a Porter-Thomas distribution is $\sqrt{2/n}$, where n is the number of states.

Even with the limited sample size, the observed ratio $S_{J=2}/S_{J=3}=3.5$ is unlikely if the true strength functions for $J=2$ and 3 are equal. However, since nonstatistical effects may be present, it seems inappropriate to extract a spin-spin potential from these data. Proton resonance data on other odd-mass targets in this region would be extremely useful to establish systematics and perhaps to allow the extraction of a value for the spin-spin potential.

VII. HIGH-SPIN PARTICLE-HOLE STATES

The prominent 4^-, 5^-, and 6^- $T=1$ states at $E_x=12.66$, 13.25, and 14.36 MeV in ^{28}Si may consist mainly of a $d_{5/2}^{-1}f_{7/2}$ p-h configuration. The 6^- stretched state is formed by $f_{7/2}$ particle transfer only, and thus is the most simply excited of the three states. The 5^- state can be formed by both $f_{5/2}$ and $f_{7/2}$ particle transfer, while the 4^- state has an additional $p_{3/2}$ component. These states possess most of the observed $l=3$ strength in ^{28}Si and have been studied through the (^{3}He,d) (Refs. 13 and 28–30), (α,t) (Ref. 31), (p,p), and (p,γ) (Refs. 13 and 32) reactions as well as by intermediate energy inelastic scattering of protons,[33] pions,[34] and electrons.[35,36] The spectroscopic factors from the resonance and proton transfer reactions are presented in Table VI along with the parent state spectroscopic factors. In order to present a unified discussion of all of the particle-hole states we observed in ^{28}Si, discussion of those states observed at lower energies was deferred. Data for the 4^- state and the strongest 5^- state appear in Ref. 1.

The 4^-, $T=1$ state occurs as a resonance[1] at $E_p=1.119$ MeV. The 4^- states may be formed by $l=1$ transfer with $j=\frac{3}{2}$ and by $l=3$ transfer with $j=\frac{5}{2}$ or $\frac{7}{2}$.

TABLE VI. Particle-hole state spectroscopic factors for ^{28}Si and ^{28}Al.

E_x (MeV)	J^π; T	l	S_p (p,p)	S_p (^{3}He,d)	S_n (d,p)
12.66	4^-; 1	1,3	0.17, <1.0[a]	0, 0.74[b]	0.11, 0.62[c]
				0, 0.42[d]	0.09, 0.58[e]
				0, 0.84[f]	0, 0.53[g]
13.25	5^-; 1	3	0.69[a]	0.59[h]	0.85[c]
				0.37[b]	0.43[e]
				0.28[d]	0.85[i]
				0.65[f]	0.66[g]
14.36	6^-; 1	3	0.68[j]	0.42[h]	0.65[i]
			0.52[k]	0.38[b]	0.36[g]
			0.62[a]	0.28[d]	
				0.34[k]	
				0.57[f] (0.4)[l]	

[a]Present work.
[b]Reference 29.
[c]Reference 23.
[d]Reference 30.
[e]Reference 24.
[f]From (α,t) in Ref. 31.
[g]From (α,^{3}He) in Ref. 31.
[h]Reference 28.
[i]Reference 25.
[j]Reference 2.
[k]Reference 13.
[l]With unbound form factor in Ref. 31.

Unfortunately the present experiment is most sensitive to the $l=1$ component due to the extremely small penetrabilities for $l=3$ at low energies. Only an upper limit could be set for the $l=3$ strength for the 4^- state. The transfer reactions are more sensitive to the $l=3$ strength, but do not determine the ratio of the $j=\frac{5}{2}$ and $\frac{7}{2}$ strengths. There is reasonable agreement between the $l=1$ strength of the present experiment and that observed in the (d,p) reactions; however, no $l=1$ strength is reported for the other transfer reactions.

The 6^- stretched state ($E_p=2.875$ MeV) presumably has the simplest structure of these $l=3$ states and is the most studied. Comparisons of the particle transfer spectroscopic factors with the inelastic spectroscopic strengths have been performed in terms of a simple particle-hole shell model.[2,13,31] The deficiencies inherent in making such a comparison have been pointed out by Emery[37] and Zamick.[38] The spectroscopic factors in Table VI may be compared directly. The first and third resonance spectroscopic factors were obtained from the value $\Gamma_p=3.7$ keV, while the second is obtained from the value $\Gamma_p=4.0$ keV of Snover. Various methods of calculating the single particle width Γ_{sp} account for the major differences in the resonance spectroscopic factors. Halderson obtained the value $\Gamma_{sp}=10.8$ keV on the basis of g-matrix considerations, while Snover *et al.* chose the range $12.6<\Gamma_{sp}<17.4$ keV from the parameters which gave acceptable DWBA fits to (^{3}He,d) data. The present value $\Gamma_{sp}=11.9$ keV results from our usual method of calculating the analog state spectroscopic factor (Sec. V).

The spectroscopic factors obtained from resonance reactions are larger than those of the transfer reactions. The reason for this discrepancy is unknown. The striking feature common to all of these measurements is that the strength is much less than that expected on the basis of a simple particle-hole shell model calculation. Amusa and Lawson[39] have performed shell model calculations with an extended basis which qualitatively explain much of the observed quenching. Two recent papers[37,38] have shown that the single particle strength is reduced if a deformed core is assumed in the calculation of the single particle strength. These model calculations also predict fragmentation of the strength to two or more states. The high resolution of the present experiment gives excellent sensitivity to such fragmentation. No other 6^- states with appreciable strength are observed in the present data for $12.5<E_x<14.9$ MeV. A comparison of the data and model calculations is currently being prepared.[40]

The 5^- "nearly stretched" states are also interesting. The major portion of the 5^-, $T=1$ strength is observed in the resonance[1] at $E_p=1.724$ MeV. Although these states are strongly excited in resonance and transfer reactions, the excitation of the 5^-, $T=1$ state is extremely weak in inelastic proton scattering.[33] The quenching of the single particle strength for the 5^- states is similar to that for the 6^- in resonance and transfer reactions. However, the 5^- strength may be split between the $E_x=13.25$ MeV level and the level at $E_x=13.98$ MeV.

It is useful to determine the relative strength for $f_{5/2}$ and $f_{7/2}$ particle transfer leading to the 5^- state. The measured value of the channel spin mixing ratio ξ provides some information. We define the total angular momentum mixing ratio as

$$T=\Gamma_{j=7/2}/(\Gamma_{j=5/2}+\Gamma_{j=7/2}) , \tag{5}$$

where Γ_j is the partial width for scattering of a particle with total angular momentum j. The relation between T and ξ is

$$T=\tfrac{1}{7}\{3\xi\pm 2[10\xi(1-\xi)]^{1/2}+2\} . \tag{6}$$

Thus a quadratic ambiguity exists in extracting the value of T from the measured value of ξ. This relationship is shown in Fig. 4. Our value of $\xi=0.65\pm0.15$ is in agreement within errors with that of Lam *et al.*[41] This value yields the two possible ranges for T: $0.95<T<1.0$ and $0.05<T<0.27$. Thus the 5^- state is either completely $f_{7/2}$ or predominantly $f_{5/2}$. A resonance measurement cannot remove this ambiguity; however, it may be possible to infer which of the two solutions is correct from analyses of the inelastic scattering data.

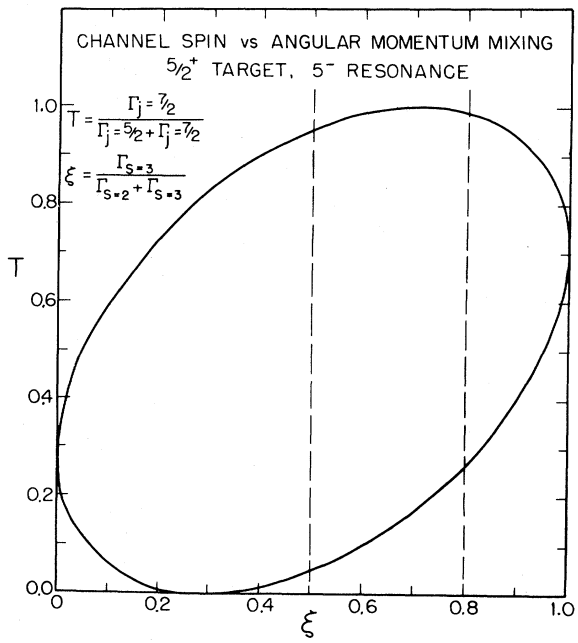

FIG. 4. The total angular momentum mixing ratio T vs the channel spin mixing ratio ξ for a $J^\pi=5^-$ state. The ellipse is given by Eq. (6). The measured value of ξ is 0.65 ± 0.15; the upper and lower limits are indicated by dashed vertical lines. Possible values of T lie on the two portions of the ellipse bounded by these dashed lines.

VIII. SUMMARY

Results from the R-matrix analysis of 73 resonances in ^{28}Si in the range $E_p=1.85$–3.05 MeV have been presented. Reasonable agreement was found with previous measurements in this energy range and much new information including l values, channel spin mixing and l-mixing ratios, partial widths, and resonance angular momenta was

extracted. The measured s-wave strength functions show a large difference between $J=2$ and $J=3$ resonances. However, more data are needed to interpret this result. No fragmentation of the 6^-, $T=1$ stretched state is observed. This result should provide a test for some of the possible explanations of the observed quenching of the single particle strength. The strength of the 5^-, $T=1$ state was also determined, and two possible total angular momentum mixing ratios were extracted from the measured channel spin mixing ratio. Proton scattering studies on other odd-mass targets are now being performed.

ACKNOWLEDGMENTS

The authors would like to thank P. M. Endt for valuable comments on the spectroscopy of ^{28}Si, and G. T. Emery, C. Olmer, K. A. Snover, and G. E. Walker for useful discussions concerning particle-hole states in ^{28}Si. The as-The assistance of J. F. Shriner, Jr., G. Adams, P. Ramakrishnan, J. Vanhoy, and B. Warthen in taking portions of these data is appreciated. This work was supported in part by the U.S. Department of Energy, Office of High Energy and Nuclear Physics, under contracts No. DE-AC05-76ER01067 and DE-AS05-76ER03624.

[1]R. O. Nelson, E. G. Bilpuch, C. R. Westerfeldt, and G. E. Mitchell, Phys. Rev. C **29**, 1656 (1984).
[2]D. Halderson *et al.*, Phys. Rev. C **24**, 786 (1981).
[3]F. C. Shoemaker *et al.*, Phys. Rev. **83**, 1011 (1951).
[4]M. A. Rahman, M. A. Awal, and M. Rahman, Lett. Nuovo Cimento **17**, 533 (1976).
[5]M. A. Abuzeid *et al.*, Nucl. Phys. **45**, 123 (1963).
[6]L. Zolnai, E. Koltay, I. Hunyadi, and B. Nyako, Izv. Akad. Nauk SSSR, Ser. Fiz. **40**, 2119 (1976) [Bull. Acad. Sci. USSR, Phys. Ser. **40**, 78 (1976)].
[7]C. C. Hsu *et al.*, J. Phys. G **3**, 1753 (1977).
[8]M. A. Meyer, I. Venter, and D. Reitmann, Nucl. Phys. **A250**, 235 (1975).
[9]J. Dalmas and D. Bertault, J. Phys. (Paris) **34**, 357 (1973).
[10]J. Dalmas, C. R. Acad. Sci. (Paris) Ser. B **277**, 237 (1973).
[11]P. M. Endt and C. Van der Leun, Nucl. Phys. **A310**, 1 (1978).
[12]J. E. Lynn, *The Theory of Neutron Resonance Reactions* (Clarendon, Oxford, 1968), pp. 274—280.
[13]K. A. Snover, G. Feldman, M. M. Hindi, and E. Kuhlmann, Phys. Rev. C **27**, 493 (1983).
[14]C. R. Westerfeldt, G. E. Mitchell, E. G. Bilpuch, and D. A. Outlaw, Nucl. Phys. **A303**, 111 (1978).
[15]E. G. Bilpuch, A. M. Lane, G. E. Mitchell, and J. D. Moses, Phys. Rep. **28**, 145 (1976).
[16]A. M. Lane and R. G. Thomas, Rev. Mod. Phys. **30**, 257 (1958).
[17]R. O. Nelson, E. G. Bilpuch, C. R. Westerfeldt, and G. E. Mitchell, Phys. Rev. C **27**, 930 (1983).
[18]C. R. Gould *et al.*, IEEE Trans. Nucl. Sci. **28**, 3708 (1981).
[19]G. F. Neal and S. T. Lam, Phys. Lett. **45B**, 127 (1973).
[20]C. Miehe, J. P. Gonidec, A. Huck, and G. Walter, Rev. Phys. Appl. **8**, 22 (1973).
[21]G. F. Neal and P. R. Chagnon, Phys. Rev. C **11**, 1461 (1975).
[22]H. L. Harney and H. A. Weidenmüller, Nucl. Phys. **A139**, 241 (1969).
[23]T. P. G. Carola and J. G. Van der Baan, Nucl. Phys. **A173**, 414 (1971).
[24]S. Chen, J. Rapaport, H. Enge, and W. W. Buechner, Nucl. Phys. **A197**, 97 (1972).
[25]R. M. Freeman, F. Haas, A. R. Achari, and R. Modjtahed-Zadeh, Phys. Rev. C **11**, 1948 (1975).
[26]M. A. Rahman *et al.*, Lett. Nuovo Cimento **12**, 290 (1975).
[27]V. P. Alfimenkov *et al.*, Nucl. Phys. **A376**, 229 (1982).
[28]S. Kato and K. Okada, J. Phys. Soc. Jpn. **50**, 1440 (1981).
[29]H. Nann, Nucl. Phys. **A376**, 61 (1982).
[30]A. Djaloeis *et al.*, Phys. Rev. C **28**, 561 (1983).
[31]M. Yasue *et al.*, Nucl. Phys. **A391**, 377 (1982).
[32]J. Dalmas, F. Leccia, and M. M. Aléonard, Phys. Rev. C **9**, 2200 (1974).
[33]G. S. Adams *et al.*, Phys. Rev. Lett. **24**, 1387 (1977).
[34]C. Olmer *et al.*, Phys. Rev. Lett. **43**, 612 (1979).
[35]S. Yen *et al.*, Phys. Lett. **93B**, 250 (1980).
[36]S. Yen *et al.*, Phys. Rev. C **27**, 1939 (1983).
[37]G. T. Emery, in Proceedings of the International Symposium on Highly Excited States and Nuclear Structure, Orsay, France, 1983.
[38]L. Zamick, Phys. Rev. C **29**, 667 (1984).
[39]A. Amusa and R. D. Lawson, Phys. Rev. Lett. **51**, 103 (1983).
[40]G. T. Emery (private communication).
[41]S. T. Lam, A. E. Litherland, and R. E. Azuma, Can. J. Phys. **49**, 689 (1971).